의학박사 학위논문

Quantitative Analysis of Ultrasound Imaging in Retinoblastoma Mouse Model

망막모세포종 생쥐모델에서 초음파 영상장비를 이용한 정량적 분석

2016 년 2 월

서울대학교 대학원

임상의과학과

유 승 호

A thesis of the Degree of Doctor of Philosophy

망막모세포종 생쥐모델에서 초음파 영상장비를 이용한 정량적 분석

Quantitative Analysis of Ultrasound Imaging in Retinoblastoma Mouse Model

Feb. 2016

The Department of
Clinical Medical Sciences,
Seoul National University
College of Medicine
Seung Ho Yoo

Abstract

Introduction: Retinoblastoma is one of the highest rate of intraocular malignancy for children's eyes. But several available treatments (Chemotherapy, radiation, thermotherapy, cryotherapy, and laser, etc) are not working well and enucleation is widely used for many cases in the end. This study is to establish an orthotopic transplantation model injecting Y79 retinoblastoma cells into the mouse eye and time differentially identify the tumor formations, growths, and drug responses using three dimensional ultrasound imaging.

Methods: First of all, the cultured Y79 retinoblastoma cells were injected into mouse eyes and the time differential quantitative analysis of tumors was performed through three dimensional ultrasound imaging. The appropriate concentration rate of anti-cancer drug (carboplatin) was calculated to identify the apoptotic cell death through MTT assay and western blotting analysis. Then, the drug was injected into the tumor models to observe the phenomena of tumors reduction through three dimensional ultrasound imaging.

Results: The tumor formations and growths were observed time differentially through three dimensional ultrasound imaging. And the apoptotic cell death was identified by anti-cancer drug (carboplatin) indicating cleaved caspase 3 through MTT assay and it was also proven with statistically meaningfulness ($p<0.05$) through western blotting analysis. Accordingly, the drug treatment was effectively identified with the result of the tumors reduction through three

dimensional ultrasound imaging.

Conclusions: Two dimensional tumor formations and growths in retinoblastoma cells have been widely observed but the tumor volume measurement was not realistic due to its difficulty and inaccuracy. This study was time differentially identified the tumors formations and growth and each tumor volume were rather precisely measured using three dimensional ultrasound imaging. Observing well established orthotopic transplantation models (in vivo) which gave us the distinctive drug responsiveness using three dimensional ultrasound imaging is fairly effective screening anti-cancer drugs and ultimately contributes to develop a new drug in the future.

Keywords: Retinoblastoma, animal model, orthotopic transplantation, ultrasound, anti-cancer drug screening

Student number: 2013-30824

CONTENTS

Abstract i

Contents iii

List of tables and figures iv

List of abbreviations v

Introduction **1**

Material and Methods **10**

Results **21**

Discussion **33**

References **36**

Abstract in Korean **41**

LIST OF TABLES AND FIGURES

Table 1 Various sound waves with each characteristics 4

Figure 1 (A) Front view of Vevo® 2100 Imaging System, (B) Transducer 6

Figure 2 Introduction of Vevo® 2100 Imaging System 7

Figure 3 Micro CT image using NFR POLARIS-G90 9

Figure 4 Mimetic diagram of the orthotopic mouse model 14

Figure 5 Mouse eye picture using a high performance camera 15

Figure 6 Procedures of ultrasound imaging (Vevo® 2100 Imaging System) 17

Figure 7 Three dimensional ultrasound imaging procedures 19

Figure 8 Cell viabilities according to the carboplatin treatment 21

Figure 9 Apoptotic cell death representing pink-colored for cleaved caspase 3 in Y79 retinoblastoma cells 22

Figure 10 Inducement of apoptotic cells death with carboplatin treatment in retinoblastoma cells 24

Figure 11 Time differential photographs in retinoblastoma mouse model between carboplatin treatment and non-treatment groups 26

Figure 12 Time differential H&E in retinoblastoma mouse model between carboplatin treatment and non-treatment groups 27

Figure 13 Tumor volume measurement using three dimensional ultrasound imaging system 29

Figure 14 Time differential retinoblastoma matches between H&E and ultrasound images 30

Figure 15 Time differential quantitative tumor changes identified by ultrasound imaging system 32

LIST OF ABBREVIATIONS

RB : Retinoblastoma

SNUH : Seoul National University Hospital

IACUC : Institutional Animal Care and Use Committee

WK : Week

FBS : Fetal Bovine Serum

MTT : 3-(4,5-dimethylthiazol-2-yl)-2,5-diphenyltetrazolium bromide

IFU : Instructions For Use

ARVO : Association for Research in Vision and Ophthalmology

MFDS : Ministry of Food and Drug Safety

PBS : Phosphate Buffer Saline

SDS-PAGE : Sodiumdodecylsulfate-polyacrylamide gel eletrophoresis

2D : Two Dimensional

3D : Three Dimensional

PET : Positron Emission Tomography

CT : Computed Tomography

MRI : Magnetic Resonance Imaging

Introduction

Eyes have an important and complex optical system as one of the critical organs in human body and it is the organ which is in charge of vision and focuses on the object through the adjustable lenses to make an image. Their main functions are to detect the light and convert it into electrical impulses in neurons. Through several types of neural system, those impulses are finally forwarded to the brain. Specifically, it connects to the eye through the optic nerve working with the cortex which is in charge of vision in the brain. Ultimately, people are able to see the objects collecting the light from the environment (1, 2).

That is why the optical system is extremely critical to human and the patient might lose their significant quality of life without the visual function caused by any hereditary reason or accidental event. Structurally in eyes, retina is a thin layer of nerve cells that make up the inner nerves surrounding the eyes in the vertebrate animals and cephalopods. Its role is mostly likely to correspond to a film of the camera. The eye development with the optic nerve and retina in vertebrates are derived from the result by the brain growth and anatomically, retina is classified as sensory apparatus and optic nerves are classified as peripheral nerves. But retina is embryologically classified as a part of Central Nervous System (3).

Human retina is generally corresponded to a film of the camera but the film that cannot compare with human retina because the retina is partly illuminated and the rest are listed as a shadow, and it does carefully identify the objects. A rod (low light-sensitive cell) in retina is able to identify the objects in the dark. When stayed in the bright place, people cannot see them in a dark area but soon adapt to the darkness distinguishing the objects with a rod. Cone cells distinguish the light and identify each red, green, and blue color. Sending those color information to brain through the optic nerve behind the retina, people can ultimately identify the color seeing the objects (4).

The most common intraocular tumors in adults are lymphoma and melanoma but retinoblastoma is one of the highest rate of intraocular malignancy in childhood. Those children who are mostly five years old or under are diagnosed with retinoblastoma and it is reported affecting one in every 20,000 approximately in US (5).

The main reason of the retinoblastoma is caused by tumor suppressor gene with dysfunctional protein. The firstly cloned eye cancer, RB1 gene is derived from homozygosity for a retinoblastoma gene mutation. The tumor can be seen mostly 75% of the time in one eye and 25% of them can be occurred in both eyes. Due to the defective gene, it is inherited from parent to their child with about 40% proportion since the defects are generally occurred at the early fetal development stage (6-8).

While many children and their parents are suffering from the cancer with sickness, there are few treatments to be cured and mostly their eye(s) salvage is required unfortunately. Even if radiotherapy with X-ray equipment can be a way to limitedly treat those patients, there are some side effects due to the radiations and it is piteous that most of them finally get the enucleation to prioritize one's life saving. Otherwise, the tumors in retina can be extended into other organs in human body and it could be life threatening. Since currently available treatments such as thermotherapy, cryotherapy, laser, and chemotherapy, etc are not so effective clinically, those children with retinoblastoma may lose their eye(s) finally (9).

This study has started for the purpose of the importance of saving children's life and longer life expectancy. Through the quantitative analysis using orthotopic transplantation tumor model, it is helpful to diagnose the retinoblastoma and observe specific tumors formation and growths. Also, this study is able to contribute to develop a new drug checking the anti-cancer drug responsiveness.

To accurately figure out the retinoblastoma and understand the tumor with angiogenesis and oncogenesis, various ways and efforts have been tried for the distinctive diagnosis. There are X-ray, Micro CT, PET-CT, MRI, and sonography, etc. and each of them have both advantages and disadvantages occurring some side effects and/or not showing clear images to be identified. However, ultrasound imaging equipment shows us clearer images with the progression of

retinoblastoma compared to other diagnostic equipment. And no sources say there are side effects or discomforts to the patients using ultrasonography (10).

Types	Frequency Band	Characteristics
Infrasound	Less than 20Hz	Lower than normal level of human hearing(For monitoring earthquake)
Sound	Between 20Hz and 20KHz	Acoustic(Low bass notes)
Ultrasound	Between 20KHz and 2MHz	Medical use and destructive
	Over 2MHz	Diagnostic purpose and Non-destructive evaluation

Table 1 : Various sound waves with each characteristics

There is a limit for human to be audible and ultrasounds are sound waves with high frequencies but physical properties are same as normal sounds. As shown on the above Table 1, ultrasound imaging systems operate with the frequencies from 20 KHz up to several giga hertz.

The ultrasound is widely useful for several fields like communication, locating, non-destructive tests, and medical purpose, etc. There are several types of devices using ultrasound detecting object and measuring the distances like animal such as bats and also usefully activated for the cleaning and chemical processing purposes. The basic principle to detect the object is to reflect any flaws using sonar energy back to the transducer that is in charge of the detection and display. Clinically, ultrasound (sonography) is often used for the diagnosis and treatment as well (11).

For this study, following ultrasound imaging equipment, Vevo® 2100 Imaging System by FUJIFILM VisualSonics, Inc. (Figure1) was used at Seoul National University Hospital Pre-clinical (Animal) Lab. It is applicable for small animals like rabbits, guinea pigs, rats, and mice using the frequencies from 12.5MHz to 45MHz. The transducer with 256 element array is featured with the frame rate over 300frames per second. According to the SNU Animal Lab Guideline and IACUC, the users were recorded for this experimental study whenever using the ultrasound imaging with mouse modeling.

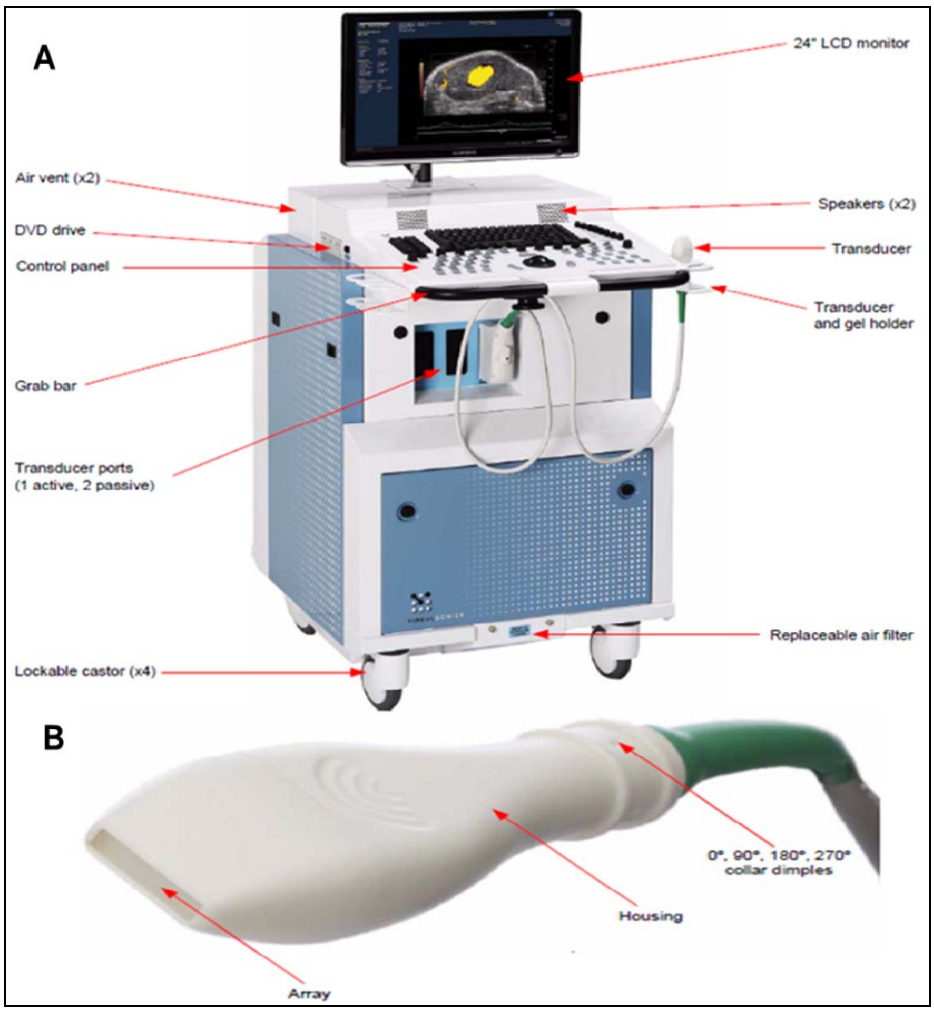

Figure 1. (A) Front view of the Vevo® 2100 Imaging System, (B) Transducer (Copyright by FUJIFILM VisualSonics, Inc.) To smoothly use the equipment and receive the best images using the Vevo® 2100 Imaging System, the technical engineer from VisualSonics Asia Pacific Regional Office was invited to SNUH Animal Lab. The engineer provided researchers with the training programs how to measure the tumor volume and use the detailed features of the equipment with three dimensional visualization, etc through three day-long trainings

and expertized meetings in Korea. The optimized images with high quality had resulted in learning through the animal staging, imaging workflow, and displays with 3D images, etc using the Vevo® 2100 Imaging System.

Figure 2. Introduction of Vevo® 2100 Imaging System. Each of the above pictures (Figure 2) shows us the Vevo® 2100 Imaging System from booting the Workstation and starting the ultrasonography to generate images of mouse eyes positioned inside the cage.

Since Wilhelm Roentgen (Professor of Physics in Wurzburg in Germany) had discovered X-ray images using electromagnetic radiation in 1865 (12), the use of x-rays have been widely spread for many areas around the world and other radiation tools have been hugely developed with outstanding improvement and innovations. While there are a lot of helpful usage and activated applications using x-rays without cutting the flesh of human body, nobody were

recognized its disadvantages until serious injuries had expressed to the human bodies in a few years. Basically, the lack of understanding using x-rays' drawbacks was the main reason to be injured to people due to the serious radiation exposures and direct contacts to the radiation and fluorescent materials, etc (13).

Through the revolutionary development with the high technologies, X-ray equipment has been evolving with CT, PET-CT, and MICRO CT, etc. Even if there are several disadvantages, they are still widely used for medical areas as a diagnostic tool and it is greatly useful for patients to get to know their symptoms with the cutting edge diagnostic technologies. Always, people needs to be careful for the overuse and/or misuse of risky radiations though (14).

There was an initial trial using In-vivo Micro CT, NFR POLARIS-G90 (NanoFocusRay Co., Ltd., Jeonju, Korea) at SNUH Animal Lab in retinoblastoma mouse model and several images came out. To have the tumor images comparison between ultrasound imaging system and Micro CT, several trials were conducted. However, it was not possible for small mice to be clearly seen with the tumor formations. Even if using a contrast medium, the tumors did not inhibit unfortunately as shown on Figure 3 and no further Micro CT imaging was tried.

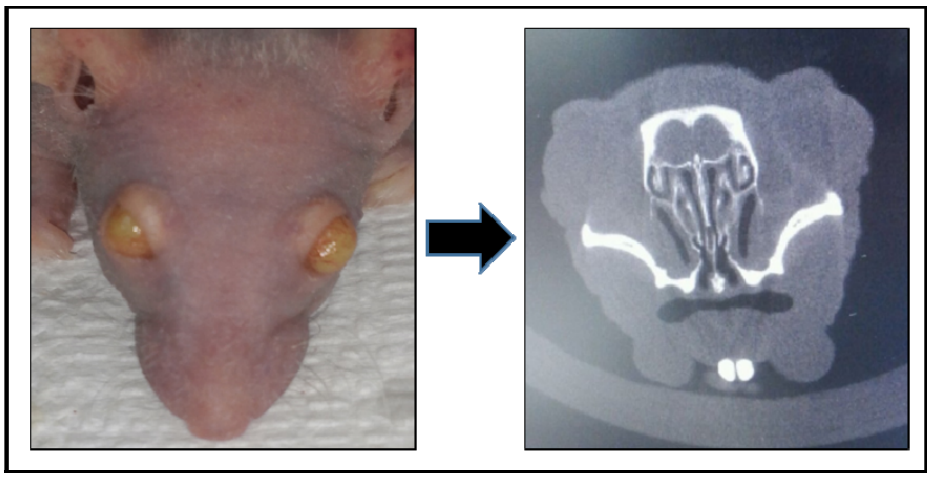

Figure 3. Micro CT image using NFR POLARIS-G90 (NanoFocusRay Co., Ltd.) The images using a contrast medium through Micro CT equipment did not show any clear images of tumor shapes and formation and no further trials were conducted.

Materials and Methods

Culture of Human Retinoblastoma Cells

Y79 cells were purchased from the American Type Culture Collection (Rockville, MD., USA) and they are human retinoblastoma cell lines being maintained in RPMI-1640 medium (WELGENE Inc., Daegu, Korea), 10% FBS (Gibco BRL, Rockville, Maryland, USA), and 100 μg/ml streptomycin (Invitrogen Life Technologies, Carlsbad, California, USA) at 37 °C in a moist atmosphere of 95% air and 5% CO_2. The medium was replaced every three day. Cultured tumor cells were observed under a phase-contrast microscope (Carl Zeiss, Chester, VA., USA) on a daily basis (15-16).

Cell Viability Assay

A cell viability was evaluated with 2-(4-Iodophenyl)-3-(4-nitrophenyl)-5-(2,4-disulfophenyl)-2H-tetrazolium (water soluble tetrazolium salt, WST-1) assay using EZ-Cytox Cell Viability Assay kit (ITSBIO, Seoul, Republic of Korea) according to the manufacturer's IFU (Instructions For Use). Y79 cells were seeded into each well of 96-well plates at a concentration of $5X10^3$ cells/well. And then the cells were treated with carboplatin (SIGMA-Aldrich, St. Louis, MO, USA) of control level at the concentrations of each 50μM, 100μM, 200μM, and 400μM for 48 hours. Then, the reagent from EZ-Cytox Cell Viability Assay kit was added to

each well. After its incubation at 37˚C for 2hours, the absorbance was measured at 450 nm/620 nm wavelength using a microplate spectrophotometer (VERSAMAX, Molecular Devices, Sunnyvale, CA) repeating four times (17-18).

Western blot analysis

Performing the standard western blotting methods, retinoblastoma (Y79) cells were treated with carboplatin (200μM) for 48hours. Combined with the controlled Y79 cells which were not treated with carboplatin could have 30μg using whole cell lysate buffer. The protein separating by 12% SDS-PAGE and then transferred into a nitro-cellulose membrane (GE) where they are stained with antibodies specific to the target protein (19). Finally, the primary antibodies (at a concentration of 1:1000 cleaved caspase 3, #9661, Cell Signaling and 1:50000 beta-actin, A2066, SIGMA) were treated overnight at 4℃ and then were removed using PBS-T solution and treated with secondary anti-body. It was exposed using EZ-Western detection kit (Daeil Lab) and the ultimate data released using LAS400 (ImageQuant™ LAS 4000: GE).

Animals

Six-week-old male BALB/c-nude mice were purchased from Central Animal Lab Inc. (Seoul, Korea) and fully managed and controlled under the conditions of 12-hour dark-light cycle and stored at

controlled room temperature (20~25℃). The environment and conditions caring, using, and treating mice in this study were strictly abided by The Association for Research in Vision and Ophthalmology (ARVO) Statement for the Use of Animals in Ophthalmic and Vision Research. Also, this study follows the Guideline by Seoul National University Institutional Animal Care and Use Committee (Approved No. 14-0024-C1A0 by SNU IACUC) in the care, use, and treatment of all animals and The Guideline of Lab Animals and Ethics by MFDS (Ministry of Food and Drug Safety).

Tumor Formation in vivo

First of all, inject the mix of Zoletil (30mg/kg) and Rumpun (10mg/kg) for anesthesia (based on an average weight : 25g/mouse) which is effective for about an hour. To induce orthotopic retinoblastoma, Y79 cells ($2x10^4$cells/$\mu\ell$ and $10x10^4$cells/$\mu\ell$) were suspended in PBS and intravitreally inoculated into each mouse eye using a 30-gauge needle and check the time differential quantitative analysis.

Tumor development was identified by indirect ophthalmoscopic examination twice a week for 4 weeks. In 4weeks of time after inoculation, the mice were killed and each eye was enucleated so that could determine whether tumors had formed with certain amount of volume and shapes. Activate ultrasound imaging equipment for the tumorigenesis with tumor volume measurement (20).

Drug responsiveness with carboplatin

For the first experiment, carboplatin (225μM : level of 75%) based on IC50 concentration (150μM) was injected to each mouse eye except for the controlled mouse after 2weeks of time with Y79 cells injection. And for the second experiment, carboplatin was injected to each mouse eye except for the controlled mouse after 10 days of time with Y79 cells injection.

After two weeks of timeframe with Y79 cells implantation, identify the regression of the tumor angiogenesis, the decreasing rate of the oncogenesis and the circumstantial tissues' infiltration level. And take a photo of each mouse eye with a high performance camera and receive the images using the ultrasound system for a comparison of tumor formations. It is repeatedly being checked at 3rd and 4th week as well. Compare the control and cases with carboplatin treated according to the time differences (21).

ICC (Immunocytochemistry)

Stick Y79 cells to DC were treated with carboplatin at a level of 200μM for 48 hours and there was a fixation with 4% paraformaldehyde for 15minutes at room temperature. The DC was incubated overnight at 4℃ with cleaved caspase 3 (1:200, Cell Signaling). Next day, the cells were treated with Alex Flour® 594 Rabbit IgG Antibody (Life Technologies) for an hour. And then DAPI (4′,6-diamidino-2-phenylindol) staining was conducted for 10 minutes (22). The color

development with cleaved caspase 3 was repeatedly identified. The cells were observed with a fluorescence microscope (Leica).

Mimetic diagram of the orthotopic transplantation mouse model

Cultivate Y79 retinoblastoma cells and stick Y79 cells to DC. And inject Y79 cells ($2x10^4$cells/$\mu\ell$) on the BALB/c-nude mice eyes and then inject anti-cancer drug, carboplatin (225μM) in 10 days. And the tumor formation will be time differentially observed by a high performance camera and ultrasound imaging every week (1^{st}~4^{th}). Finally, each tumor volume will be quantitatively measured (1^{st} experiment with 12 eyes and 2^{nd} experiment with 24 eyes were implemented).

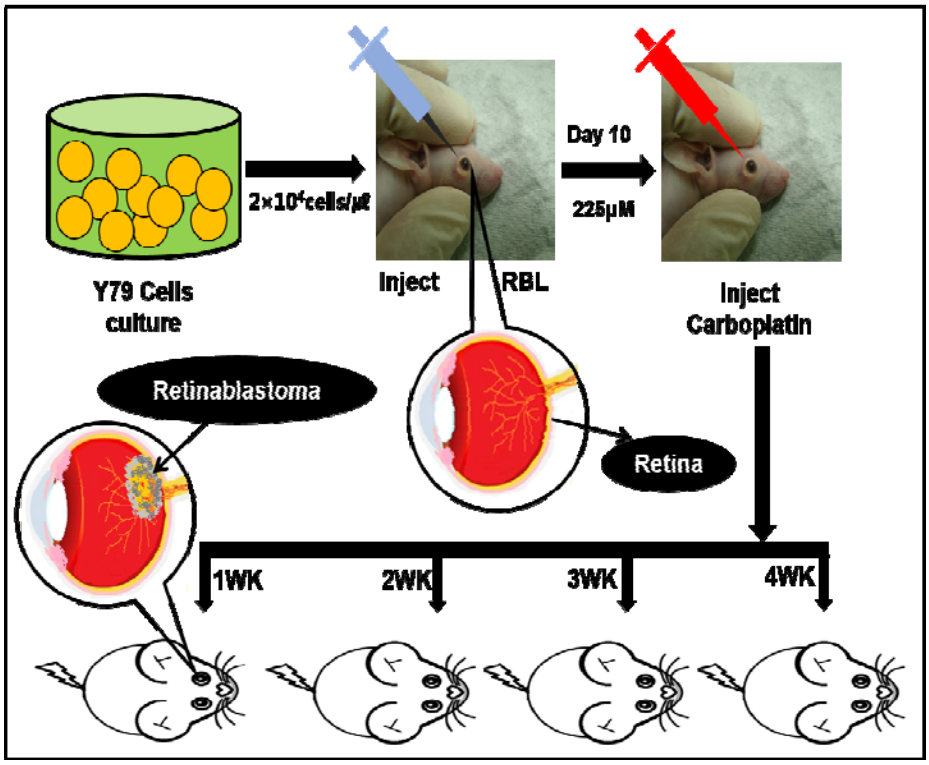

Figure 4. Mimetic diagram of the orthotopic transplantation

mouse model. After injecting Y79 retinoblastoma cells into the mice eyes and observe the tumor shapes and growths compared to the anti-cancer drug (carboplatin) treatment groups on a weekly basis for four weeks.

Photographs of mouse eye

Under the controlled environment minimizing the exposure and preventing the reflection of light, first of all carefully spread each upper and lower eyelid using fingers to have clear images of each mouse eyeball and take photographs of each mouse eye using a high performance camera.

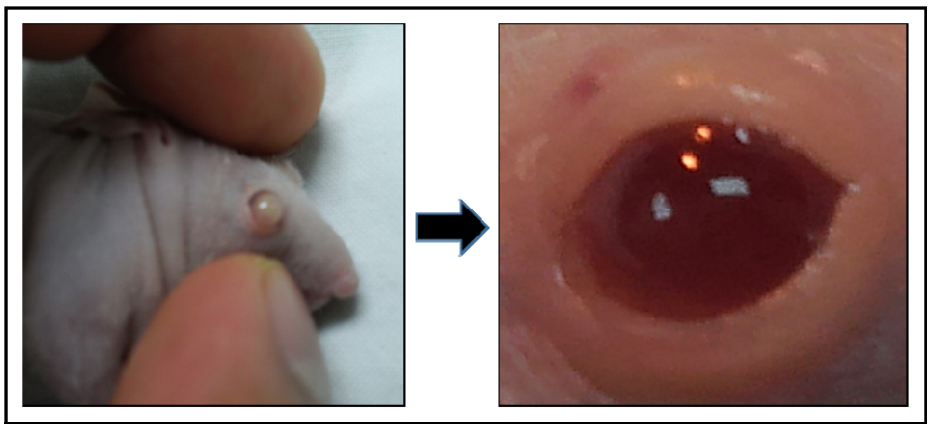

Figure 5. Mouse eye picture using a high performance camera. Take photographs of each mouse eye spreading their eyelid to have bigger and clearer images of eyeball minimizing the exposures and reflection of light.

Ultrasound (Sonography) imaging

Place each mouse on the staging platform and stage the gauze on the platform and place the anesthetized mouse on it inside the cage and then tape the eyelids (either ways) to be fixed for better and clearer images. And then ultrasound transmission ultrasound transmission gel needs to be ready under the slightly warm condition and another gauze should be covered the mouse to avoid the mouse' unexpected movement due to the coldness. Next, squeeze the ultrasound transmission gel fully overflowing on the array of the transducer (Figure 6A). And apply the ultrasound transmission ultrasound transmission gel on the mouse eye. For an important tip, an overflowing amount of ultrasound transmission gel needs to be added on the transducer cavity without any bubbles since the ultrasound transmission gel has both functions firstly to transmit ultrasound and secondly effective coupling of the light to the animal target. That is why sufficiently overflowing ultrasound transmission gel should be ready on the transducer array part to avoid any reflection and/or refraction of the light away from the animal target. If there are bubbles, reapply the ultrasound transmission gel which can remove the bubbles and it needs to be repeated until the best condition for the ultrasound imaging scan is ready. When the light is completely coupled to the target with the overfilled amount of ultrasound transmission gel, ultrasound imaging can be set smoothly using the photoacoustic sound (Figure 6B). Next, start the actual ultrasound imaging process. When

the mouse is properly positioned and the transducer with sufficient ultrasound transmission gel is ready to start the imaging process, the accurate methods to take a photograph on the mouse eye using the transducer. Firstly, it is critical to understand where the laser light comes from. It is actually from slightly out-of-plane on both sides of the ultrasound beam and then the two light gather within the photoacoustic image plane between 9 and 11mm. The light is delivered by optical fiber which is located in both sides of the transducer array part. For an important point, the animal skin line ensures to be horizontal on the ultrasound image. Specifically, the image depth, depth offset and image width, etc are adjustable using zoom-in feature. To have the consistent clear image with high quality, the depth of light penetration and the way to take the photo using the transducer array is critically important (Figure 6C).

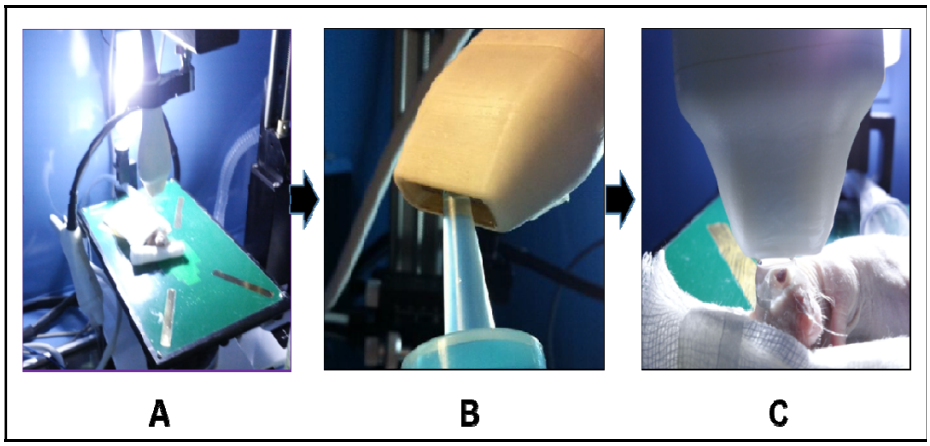

Figure 6. Procedures of ultrasound imaging (Vevo® 2100 Imaging System). Place the mouse on the staging platform and fix it with the gauzes and tapes. And sufficiently stick the ultrasound imaging gel (in

a warm condition avoiding mouse movement) on the array part of the transducer. According to IFU (instruction for use) of Vevo® 2100 Imaging System, start the ultrasound imaging scanning process.

Ultrasound imaging with three dimensional visualizations.

The first pictures by Vevo® 2100 Imaging System (FUJIFILM Visual Sonics, Inc.) were filmed from 0.4 mm mark the area, at every 15 to 20 intervals for every model for three-dimensional shape of tumors. Tumor volume measurements made after three-dimensional shape repeatedly putting a dot and drag it into the next dot and drop. Repeat the procedures to continuously draw the line with the links and will make the overall connected two dimensional areas with the specific measurement by the system. Several trials with two dimensional drawings make the three dimensional volumes possibly by x-axis, y-axis, and z-axis and the system automatically measures the actual volume. Finally, the total tumor volume is measured as we see on the captured screen.

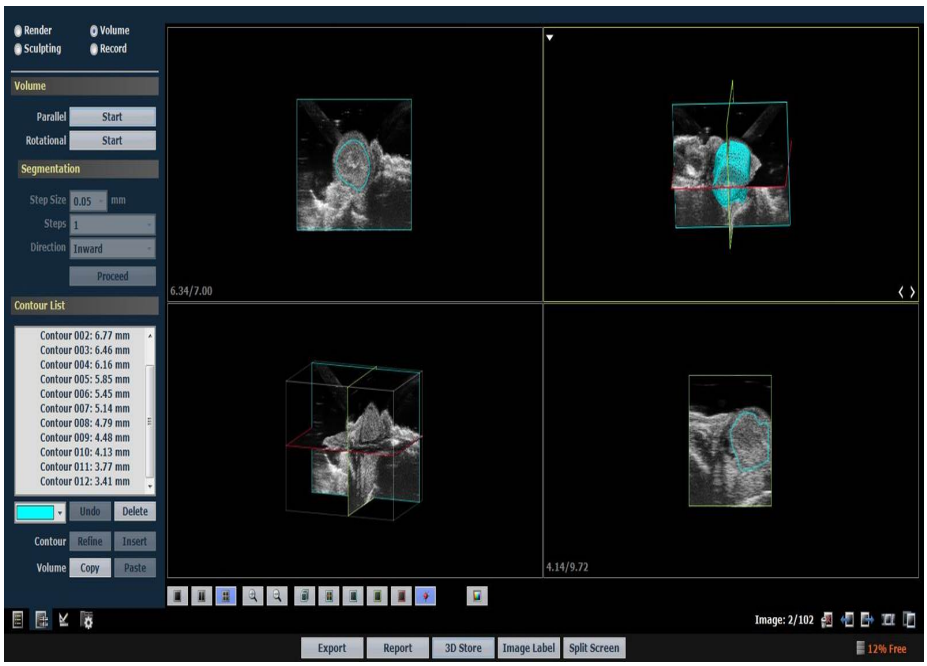

Figure 7. Three dimensional ultrasound imaging procedures (Captured image on Vevo® 2100 Imaging System). About fifteen to twenty slices with the area measurements from two dimensional ultrasound imaging process were integrated into three dimensional visualization repeatedly putting a dot and drag for a continuous line drawing with a link. It automatically calculates the total tumor volume merged by x-axis, y-axis, and z-axis as a three dimensional image (23-26).

Image analysis and statistical analysis

Each picture of the dyed retina was consolidated using Photoshop (version 6; Adobe Systems Inc., San Jose, California, USA) and analyzed the amount of tumor volume. And t-test and standard error were measured and the graph was made using GraphPad Prism

(Version 5.0; GraphPad Software Inc., San Diego, California, USA).

Its statistical analysis was performed using SPSS version 12.0 for Windows. The cut-off value of statistical significance was set at $p < 0.05$.

RESULTS

Inducement of apoptotic cells death with carboplatin treatment in Y79 retinoblastoma cells

The human retinoblastoma Y79 cell lines were established in culture and respective growth properties and changes in cells adhesion were exhibited. After being treated with carboplatin for 48hours, cell viabilities were observed and quantified by a cell proliferation assay, WST-1 (ROCHE, Switzerland). This experiment was repeated three times (* $p<0.05$). Noticeably, the reduction of cell viabilities has been started at the concentration of carboplatin (200μM) and cell viabilities were significantly reduced at the concentration of carboplatin (400μM) which means the high rate of cells death (Figure 8).

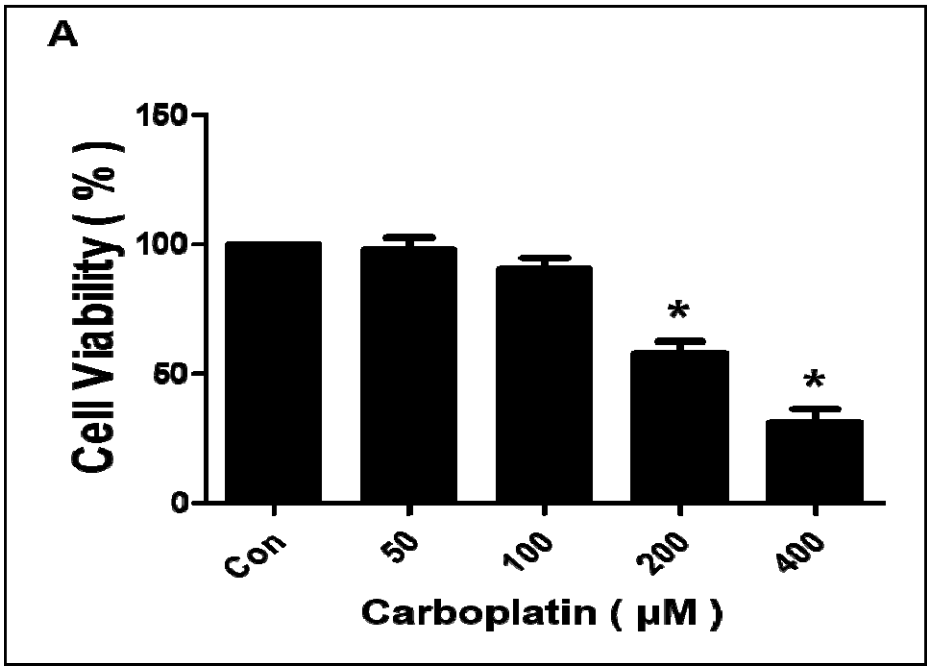

Figure 8. Cell viabilities according to the carboplatin treatment. At

the concentration of carboplatin (200μM), cell viabilities prominently reduced and then cell viabilities were lower than 30% when treated with carboplatin (400μM). It actually means the apoptotic cells death (27-28).

After the nuclear staining on Y79 cells, the nuclear morphology was identified through DAPI (4,6-diamidino-2-phenylindole) staining but there were no exhibition of any differences. Then, Y79 retinoblastoma cells were treated with carboplatin (200μM) for 48h and finally cleaved caspase 3 was observed through Immunocytochemistry which were specifically visualized the protein with pink-colored using fluorescent microscope (scale bar, 20 μm). This expression and activities were determined by western blotting analysis repeated three times (Figure 9).

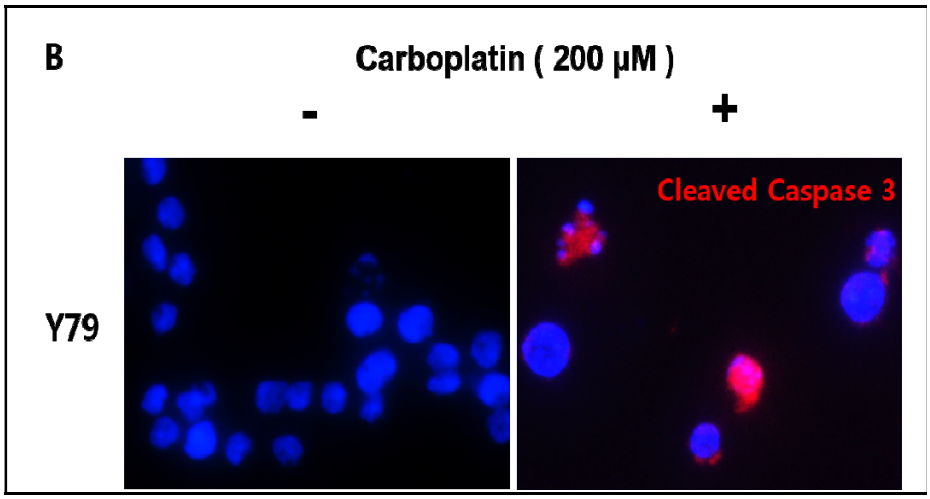

Figure 9. Apoptotic cell death representing pink-colored for cleaved caspase 3 in Y79 retinoblastoma cells. When initially

conducted DAPI staining, there was no cleaved caspase 3 exhibited but cleaved caspase 3 with carboplatin treatment was expressed with pink-colored using fluorescent microscope (Scale bar, 20 μm).

The expression of cleaved caspase 3 was derived from carboplatin treatment in Y79 retinoblastoma cells while the western blotting analysis and β-actin staining were also performed three times repeatedly (*$p<0.05$). Clearly, the representation of cleaved caspase 3 was observed about 3.8 times higher than before (29).

Comprehensively, the toxicity of the cells with each carboplatin (200 & 400μM) against the control was observed. It clearly shows us the viable cells are reducing and means getting dying. Viable cell rate 100% means that cells are alive but cells are dying due to carboplatin (200μM) effect.

In conclusion, it shows us positive cells from the carboplatin treated group and took the photos as below (pink-colored). It is proven to be the phenomena of apoptotic cells death process by anti-cancer drug effect in Y79 retinoblastoma cells (30).

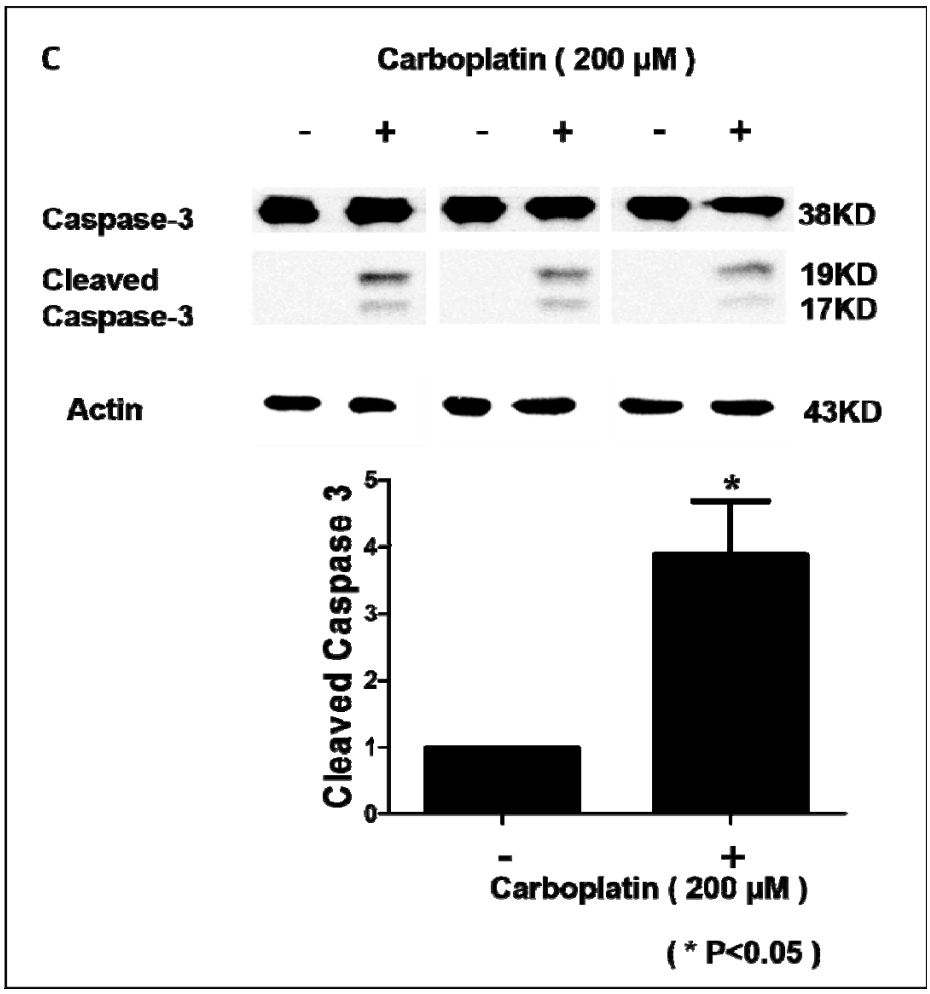

Figure 10. Inducement of apoptotic cells death with carboplatin treatment in retinoblastoma cells When treated with carboplatin (200μM), cleaved caspase 3 was observed about 3.8 times higher than non-treatment group. It is proven with the phenomena of the apoptotic cell death.

Photographs of mouse eyes with anti-cancer drug responsiveness

After Y79 retinoblastoma cells ($2x10^4$cells/$\mu\ell$) were injected into nude mouse eyes, each eye's tumor formation and shapes were monitored and recorded taking the photographs using a high performance camera every 2^{nd}, 3^{rd}, and 4^{th} week. Simultaneously, those Y79 retinoblastoma cells transplanted mouse models with carboplatin treatment groups were also monitored and taken the pictures on a weekly basis as well. Time differentially, the mouse eyes were seen as the opacity of vitreous body due to the tumor growth and full amount of the tumors into the mouse eye were observed at the 4^{th} week. However, the tumors seem to be gradually reduced for the carboplatin (225μM) treatment groups at the 2^{nd}, 3^{rd}, and 4^{th} week (Figure 11).

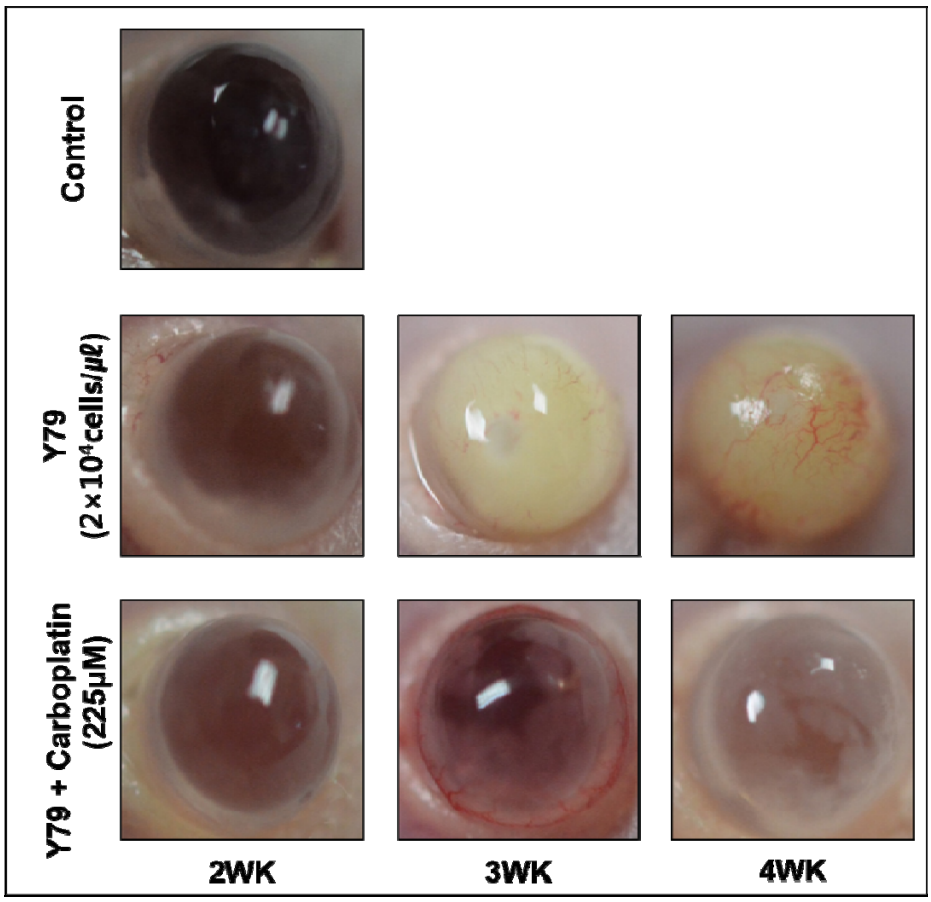

Figure 11. Time differential photographs in retinoblastoma mouse model between carboplatin treatment and non-treatment groups

Mouse eye looks opaque and hazy time differentially when Y79 retinoblastoma cells were injected. But it looks the tumors are getting reduced due to the carboplatin effect.

H&E (hematoxylin and eosin) stain of mouse eye with retinoblastoma cells.

After injecting Y79 cells (2x10^{4}cells/$\mu\ell$) to the nude mouse eye, tumor formation was checked through H&E staining every 2nd, 3rd, and 4th

week. After treating with carboplatin (225μM) in 10 days, each extracted eye was also confirmed by H&E (Scale bars, 500 μm). For the purpose of anti-cancer drug responsiveness, it was proven that the tumor mass was distinctively reduced due to the carboplatin injections. This H&E staining process ensures the retinoblastoma tumor progression and optic nerve invasion as well (Figure 12).

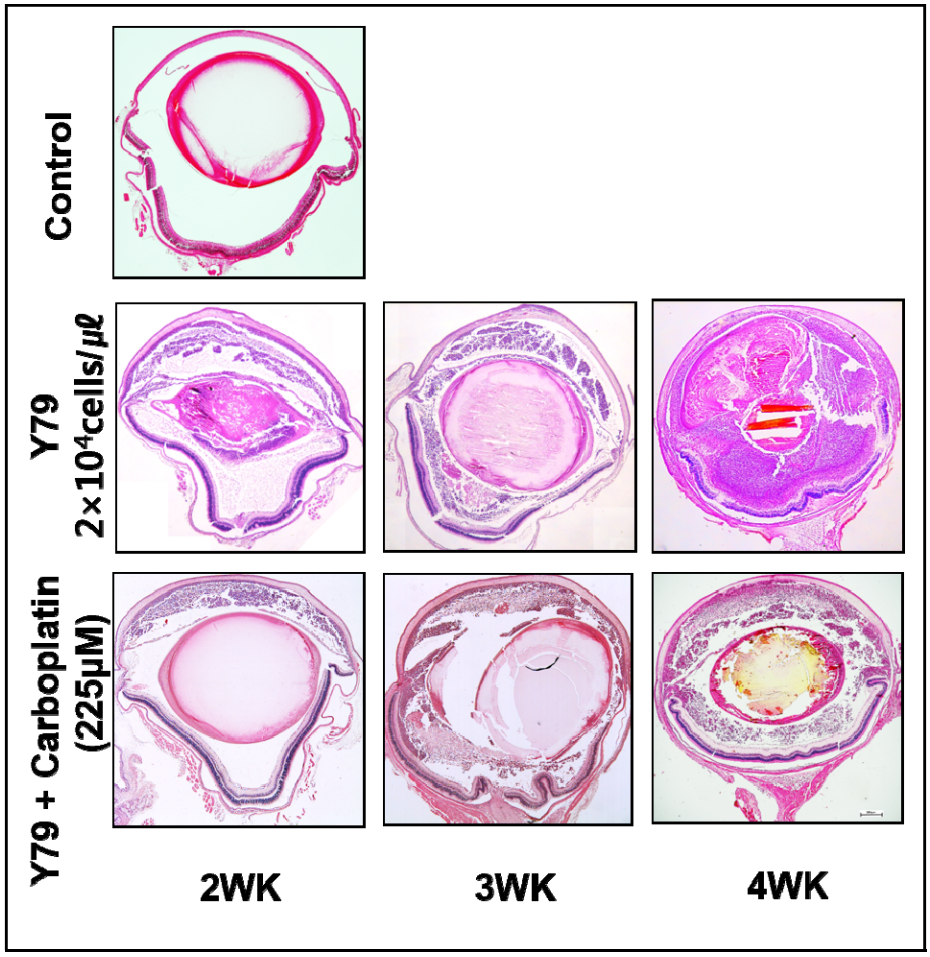

Figure 12. Time differential H&E in retinoblastoma mouse model between carboplatin treatment and non-treatment groups When Y79 retinoblastoma cells (2x10^{4}cells/$\mu\ell$) were injected in to the mouse

eye, the tumors were filled into the eyes time differentially and eyeball is fully expanded and optic nerves were also invasive with tumors due to the tumors extension. By the way, the tumor volume prominently seems to be reduced when treated with carboplatin (225μM).

Three dimensional tumor volume measurement using ultrasound imaging system.

Three dimensional ultrasound imaging system (Vevo® 2100 Imaging System from FUJIFILM VisualSonics, Inc.) effectively shows us 3D visualizations converted from two dimensional images which were filmed from 0.4 mm mark the area, at every 15 to 20 intervals. Specifically, each shape of tumors per slice are integrated into one 3D image (each surface area from x, y and z-axis). The ultrasound images basically represent the real-time based precise and sequential images with high resolution which are advantageous compared to other imaging tools such as CT and MRI, etc. Actually, there are some discrepancies and difficulties from the conventional volume measurement methods based on two dimensional images but 3D images have much easier and better visualization with more accurate volume measurement (Figure 13).

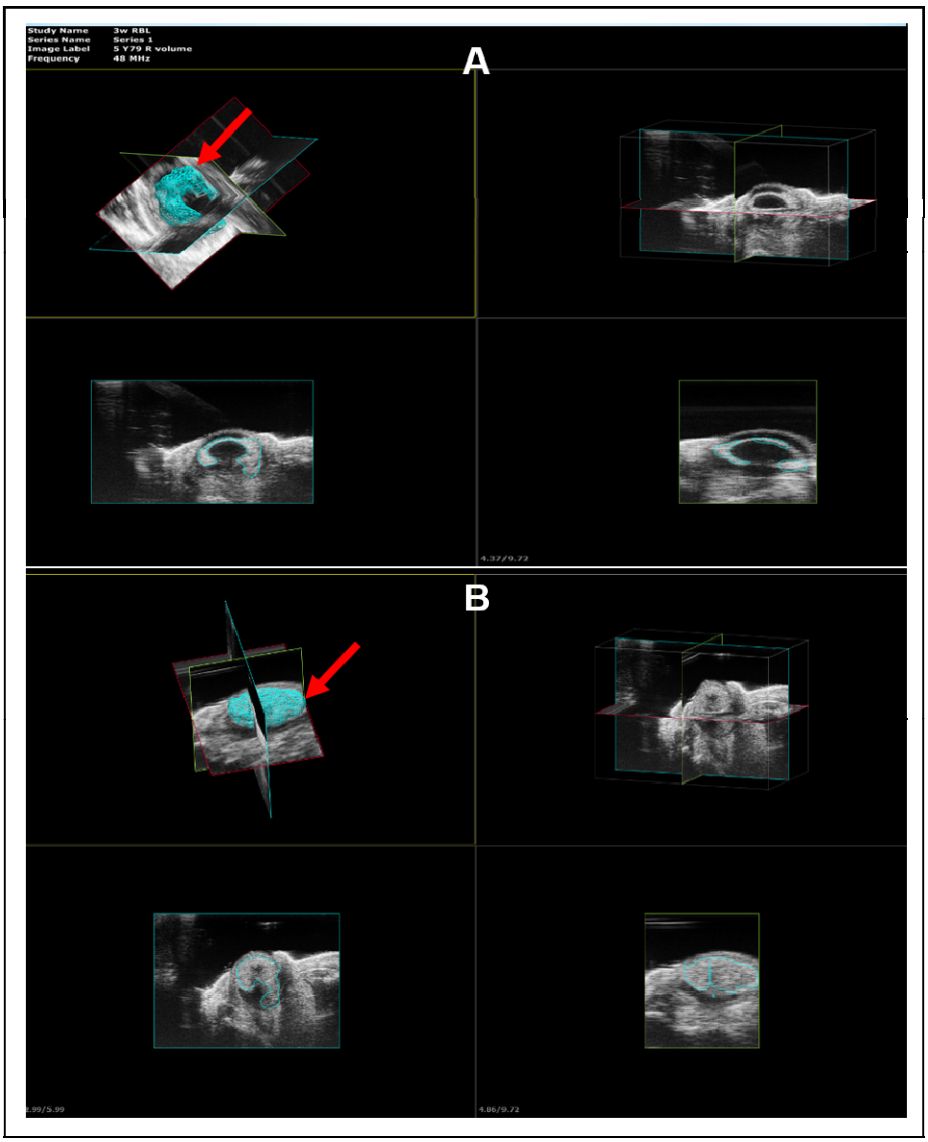

Figure 13. Tumor volume measurement using three dimensional ultrasound imaging system Both (A) and (B) clearly indicate three dimensional tumor volume which are converted from each surface area based on x, y, and z-axis. Each scanned 2D slice per 0.4 mm at with 15~20 intervals from each axis was integrated into one 3D image (red-colored arrow (A) and (B)) which are clearly shown us the tumors with the precise volume.

Time differential retinoblastoma growths are observed by both H&E stain and ultrasound imaging system.

H&E section clearly shows us each part of eyeball with tumor shapes and growth every week. The tumor extension into the optic nerves is also observed and vitreous body keep shrinking due to the tumor expansion. At the same time, the ultrasound images inhibits the tumor growth at the 2nd, 3rd, and 4th week. That is why two methods are popularly used to have the clear images (Figure 14).

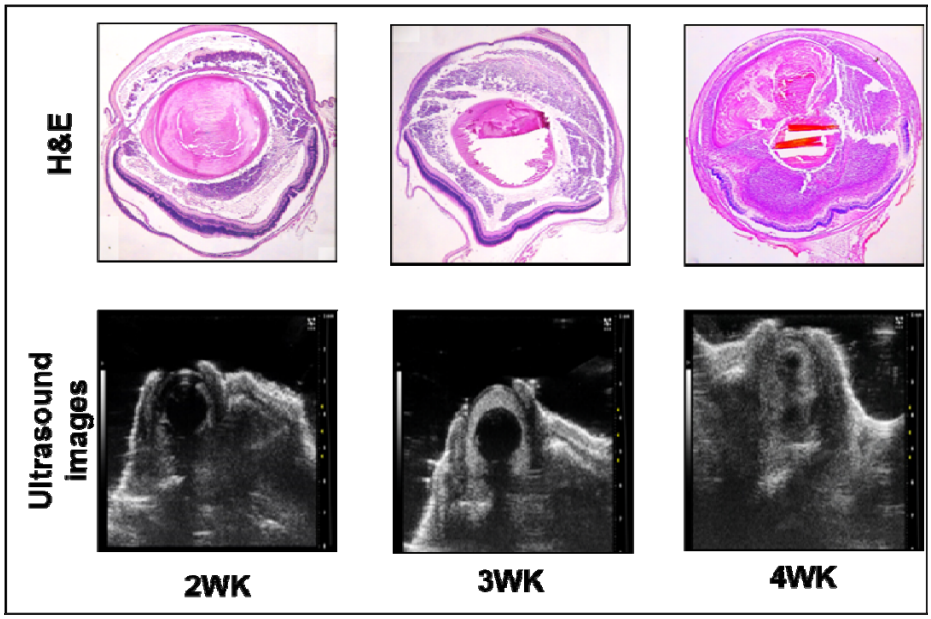

Figure 14. Time differential retinoblastoma matches between H&E and ultrasound images As time goes by, the tumor volume of the mouse eye was observed with the gradual increase every week. Both H&E and ultrasound images clearly represent the tumor growths and even being invasive into the optic nerve due to the tumor expansion while vitreous body shrinks.

Time differential tumor volume comparison between carboplatin treatment and non-treatment groups.

When injected Y79 ($2x10^4$cells/$\mu\ell$) into mouse eye, the tumor growth has been identified and tumor reductions with the carboplatin (225μM) treatment were observed every week. The initially measured tumor volume in 2weeks after Y79 cells was represented with 7.158mm^3 but the carboplatin treated group in 2weeks after Y79 injection was indicated with 4.068mm^3. And then, the tumor volume showed us with 11.613 mm^3 at the 3rd week after Y79 injection but distinctively decreased with 6.385 mm^3 for the carboplatin treatment group. When it comes to the 4th week, the tumor volume was measured with 15.036 mm^3 but the tumor volume was 9.142 mm^3 with the carboplatin treatment (Figure 15). For a reference, there is a limitation that only scans one way to be horizontal with skin when this ultrasound imaging system.

In conclusion, the tumor growths and reductions patterns were clearly inhibited with the anti-cancer drug (carboplatin) effects time differentially. And three dimensional ultrasound imaging is a relatively good method showing the statistical effectiveness ($p<0.05$) and distinctive visualizations. Above all, the tumor volume method is more accurate and convenient than other conventional methods.

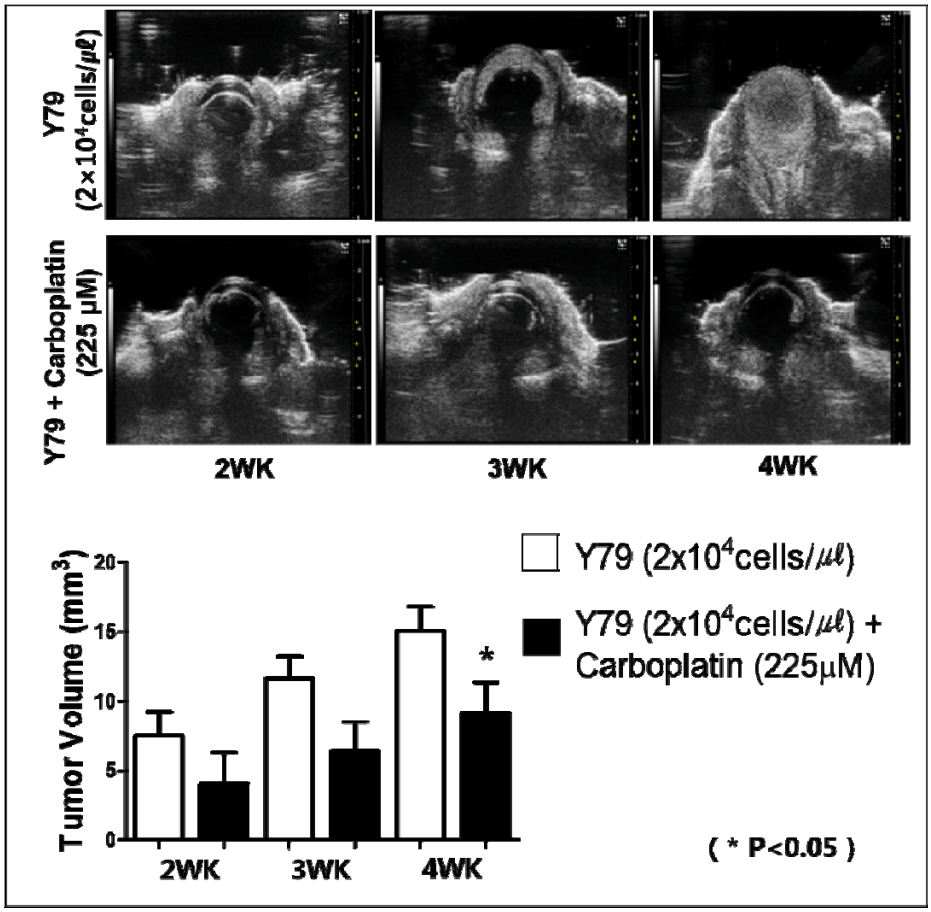

Figure 15. Time differential quantitative retinoblastoma changes identified by ultrasound imaging system. Clearly, tumors have been growing up every week and simultaneously those tumors with carboplatin treatment were shrinking. Using the convenient tumor volume measurement by ultrasound imaging system, the above graph prominently exhibits the tumor changes with statistical effectiveness on a weekly basis.

Discussion

Retinoblastoma is the most common malignant tumor of the retina in childhood. And mostly it is initiated by mutation or inactivation of the *RB1* gene which was the first described tumor-suppressor gene. Retinoblastoma is an aggressive tumor that can lead to the loss of vision, loss of the eye, and in extreme cases, to death. The degree of the tumor population was dependent on the number of Y79 retinoblastoma cells injected (5-7).

To observe well established orthotopic transplantation models under in vivo condition may enable to identify certain mutations in the RB1 genes are associated with tumor growth and subsequent cancer development. Actually, there is a limit for an ophthalmologist to qualitatively evaluate the retinoblastoma of one's eye and the quantitative analysis is inevitable to accurately investigate the tumor condition with the volume. If the RB diagnosis is delayed for 6months, the mortality rate will be increased by 70% and there is a risk for RB patient to have another cancer which is fatal especially for young children. That is why the biomarker for RB detection at an early stage is critically important and the key to scrutinize the tumor growth and development indeed. Once the biomarker has been found and early diagnosis and treatment should be followed minimizing the migration of RB and increasing the cure effect and survival rate (31-32).

For the diagnosis and imaging realization, there are various tools

such as X-ray, Micro CT, PET-CT, MRI, and ultrasound imaging system, etc. By the way, there are side effects due to the radiations and CT equipment has a limit to exhibit clear images with the progression of retinoblastoma. Also, MRI is limitedly used because of the high cost and time consumption and is not effective for children.

More importantly, the laser, thermo-therapy, cryo-therapy, and chemo-therapy in conjunction with focal therapies have been investigated for the therapeutic usage. But many RB patients unfortunately got the enucleation which is extremely painful for the patients and their family even if they received those therapies. It still remains a sight- and life-threatening ocular malignancy throughout the world.

By the way, the ultrasound imaging system is easy and convenient imaging tool to identify living tissues and show us non-invasive images of ocular structure without cross section. It inhibits real-time, rapid, and clear images with multiple slices per B-scan which is two dimensional. That is why it is beneficial to clearly have in vivo images repeatedly and sequentially through the visualization of the biological system. Above all, it allows us to have the high resolution of the images from the small animals' small tumors with the specific tumor volume. The two dimensional images per slice are integrated into one 3D image which is more accurate and quantitatively measurable of the tumor volume compared to other imaging tools. In addition, there are no side effects not causing a problem to the patients (33).

Through this study using the orthotopic transplantation mouse model, the distinctive drug responses using three dimensional ultrasound imaging were also identified which is fairly effective for us to screen anti-cancer drugs. Having a better understandings of the tumor formation and growths with those images using three dimensional ultrasound system, it may provide a useful information to develop a new anti-cancer drug. Even if it is not actually used at the clinic, it could be helpful to contribute to certain selective medication and treatment through the orthotopic tumor model.

Still, the ultrasound imaging system needs to be improved for more accurate diagnosis of the tumor volume scanning the animal in two ways at least. It still depends on the manual mapping skills by a user and the limitation is not to reflect the intraocular structure specifically. It is important to develop some clinically useful images not causing any discomfort to those patients who are suffering from the cancer and the improved treatment method and anti-cancer drug with one's life saving need to be developed accordingly.

CONFLICT OF INTEREST

There are no conflict of interests regarding this study and authors.

REFERENCES

1. SOLIMAN, Omar S., et al. Automatic localization and boundary detection of retina in images using basic image processing filters. In: Proceedings of the Third International Conference on Intelligent Human Computer Interaction (IHCI 2011), Prague, Czech Republic, August, 2011. Springer Berlin Heidelberg, 2013. p. 169-182.
2. BERROL, Cynthia F. Neuroscience meets dance/movement therapy: Mirror neurons, the therapeutic process and empathy. The Arts in Psychotherapy, 2006, 33.4: 302-315.
3. DOWLING, John E.; BOYCOTT, Brian B. Neural connections of the retina: fine structure of the inner plexiform layer. In: Cold Spring Harbor symposia on quantitative biology. Cold Spring Harbor Laboratory Press, 1965. p. 393-402.
4. CARTER-DAWSON, Louvenia D.; LAVAIL, Matthew M. Rods and cones in the mouse retina. II. Autoradiographic analysis of cell generation using tritiated thymidine. Journal of Comparative Neurology, 1979, 188.2: 263-272.
5. DEVESA, Susan S. The incidence of retinoblastoma. American journal of ophthalmology, 1975, 80.2: 263-265.
6. WEINBERG, Robert A. Tumor suppressor genes. Science, 1991, 254.5035: 1138-1146.

7. LIU, Shan-Shan, et al. Plasma microRNA-320, microRNA-let-7e and microRNA-21 as novel potential biomarkers for the detection of retinoblastoma. Biomedical reports, 2014, 2.3: 424-428.
8. DIMARAS, Helen, et al. Retinoblastoma. The Lancet, 2012, 379.9824: 1436-1446.
9. SHIELDS, C. L.; SHIELDS, J. A. Recent developments in the management of retinoblastoma. Journal of pediatric ophthalmology and strabismus, 1998, 36.1: 8-18; quiz 35-6.
10. ABRAMSON, David H. Retinoblastoma in the 20th century: past success and future challenges. Invest Ophthalmol Vis Sci, 2005, 46: 2684-91.
11. SWERDLOW, A. J. Health Effects of Exposure to Ultrasound and Infrasound. Health Protection Agency, Warsaw, 2003.
12. DONYA, Mohamed, et al. Radiation in medicine: Origins, risks and aspirations. Global cardiology science & practice, 2014, 2014.4: 437.
13. ECKERT, William G.; GARLAND, Neil. The history of the forensic application in radiology. The American journal of forensic medicine and pathology, 1984, 5.1: 53-56.
14. FORSSELL-ARONSSON, Eva, et al. Medical imaging for improved tumour characterization, delineation and treatment verification. Acta Oncologica, 2002, 41.7: 604-614.
15. LEE, Eun Kyoung, et al. NK Cell-associated Antigen Expression in Retinoblastoma Animal Model. Cancer investigation, 2013, 31.1:

67-73.

16. KIM, Jeong Hun, et al. N-myc amplification was rarely detected by fluorescence in situ hybridization in retinoblastoma. Human pathology, 2008, 39.8: 1172-1175.
17. LEE, Byung Joo, et al. Nuclear expression of p53 in mature tumor endothelium of retinoblastoma. Oncology reports, 2014, 32.2: 801-807.
18. KIM, Jeong Hun, et al. Establishment and characterization of a novel, spontaneously immortalized retinoblastoma cell line with adherent growth. International journal of oncology, 2007, 31.3: 585-592.
19. KIM, Jeong Hun, et al. Anti-tumor activity of arginine deiminase via arginine deprivation in retinoblastoma. Oncology reports, 2007, 18.6: 1373-1377.
20. JO, Dong Hyun, et al. Orthotopic transplantation of retinoblastoma cells into vitreous cavity of zebrafish for screening of anticancer drugs. Mol Cancer, 2013, 12: 71.
21. QADDOUMI, Ibrahim, et al. Carboplatin-associated ototoxicity in children with retinoblastoma. Journal of Clinical Oncology, 2012, 30.10: 1034-1041.
22. BIANCARDI, Alessandro, et al. An investigation of the photophysical properties of minor groove bound and intercalated DAPI through quantum-mechanical and spectroscopic tools. Physical Chemistry Chemical Physics, 2013, 15.13: 4596-4603..

23. HENEWEER, Carola, et al. Magnitude of enhanced permeability and retention effect in tumors with different phenotypes: 89Zr-albumin as a model system. Journal of Nuclear Medicine, 2011, 52.4: 625-633.
24. TEITZ, Tal, et al. Preclinical models for neuroblastoma: establishing a baseline for treatment. PloS one, 2011, 6.4: e19133.
25. FOSTER, F. Stuart, et al. Principles and applications of ultrasound backscatter microscopy. Ultrasonics, Ferroelectrics, and Frequency Control, IEEE Transactions on, 1993, 40.5: 608-617.
26. ZHANG, Qing, et al. In vivo high-frequency, contrast-enhanced ultrasonography of uveal melanoma in mice: imaging features and histopathologic correlations. Investigative ophthalmology & visual science, 2011, 52.5: 2662.
27. GIULIANO, Michela, et al. The apoptotic effects and synergistic interaction of sodium butyrate and MG132 in human retinoblastoma Y79 cells. Cancer research, 1999, 59.21: 5586-5595.
28. Di Fiore, R., Drago-Ferrante, R., D'Anneo, A., Auultrasound transmission gel lo, G., Carlisi, D., De Blasio, A., ... & Vento, R. (2013). In human retinoblastoma Y79 cells okadaic acid–parthenolide co-treatment induces synergistic apoptotic effects, with PTEN as a key player. Cancer biology & therapy, 14(10), 922-931.

29. KONDRIKOV, Dmitry, et al. β-Actin association with endothelial nitric-oxide synthase modulates nitric oxide and superoxide generation from the enzyme. Journal of Biological Chemistry, 2010, 285.7: 4319-4327.
30. QUAST, SA1; BERGER, A.; EBERLE, J. ROS-dependent phosphorylation of Bax by wortmannin sensitizes melanoma cells for TRAIL-induced apoptosis. Cell death & disease, 2013, 4.10: e839.
31. DOWNEY, Dónal B., et al. Three-dimensional ultrasound imaging of the eye. Eye, 1996, 10.1: 75-81.
32. FOSTER, F. Stuart, et al. Principles and applications of ultrasound backscatter microscopy. Ultrasonics, Ferroelectrics, and Frequency Control, IEEE Transactions on, 1993, 40.5: 608-617.
33. PAVLIN, Charles J.; FOSTER, F. Stuart. Ultrasound biomicroscopy: high-frequency ultrasound imaging of the eye at microscopic resolution. Radiologic Clinics of North America, 1998, 36.6: 1047-1058.

국문 초록

서론: 망막모세포종은 아이들의 눈에 발생하는 안구 내 악성종양이다. 하지만 현존하는 여러 치료법 (항암 화학 요법, 방사선치료, 온열요법, 및 냉동응고술 등)이 아주 효과적이지는 않아 결국 많은 사례에서 안구적출을 하고 있다. 본 연구에서는 망막모세포종 세포 (Y79)를 생쥐의 안구에 이식하여 종양모델을 확립하고, 3 차원 초음파 영상장비를 통해 항암제 처리군과 비교하여 시간변화에 따른 종양의 형성과정과 모양 및 부피 등을 확인 하고자 한다.

방법: 배양한 망막모세포종 (Y79)을 생쥐안구에 주입한 후 시간변화에 따른 종양의 모양과 부피를 3 차원 초음파 영상 이미지를 통해 정량분석을 실시한다. 이때 항암제인 carboplatin 을 사용하여 MTT assay 와 Western blotting 분석을 통해 세포자멸사를 확인하기 위한 적정 농도를 구하였고, 이를 종양 모델에 주사하여 항암제 반응에 따른 종양의 감소정도를 3 차원 초음파 장비를 통해 측정한다.

결과: 우선 3 차원 초음파 영상장비를 사용하여 동소이식모델의 시간변화에 따른 종양 모양 및 성장과정을 확인할 수 있었다. 항암제인 카보플라틴을 사용하여 MTT assay를 통해 cleaved caspase 3가 발현되며, 세포자멸사를 확인하였고, 아울러 western

blotting 분석을 통해 통계적으로 유의함을 입증하였다 ($p<0.05$)

따라서, 항암제가 종양 감소에 효과적임을 3차원 초음파 영상장비를 통해 확인하였다.

결론: 망막모세포종의 경우 그 동안 2 차원적인 종양모양과 성장과정만이 확인되었으며, 종양의 실제 부피를 측정하는 것은 현실적으로 불가능하였다. 본 연구에서는 3 차원 초음파 영상장비를 사용하여 시간변화에 따른 종양의 모양 및 성장과정을 확인하고, 부피를 측정할 수 있었다. 또한, 항암제에 대한 반응이 잘 확립된 동소이식모델을 3 차원 초음파 영상장비를 사용하여 관찰하여 망막모세포종에 대한 상세한 관찰 및 추적이 가능하고, 궁극적으로 새로운 항암제 선별검사에 효율적으로 이용될 수 있을 것으로 기대된다.

주요어: 망막모세포종, 동물모델, 동소이식, 초음파, 항암제 선별검사

학번: 2013-30824